JLB

Article

Biogenesis of secretory organelles during B cell differentiation

Semra J. Kirk,[1] Jacqueline M. Cliff, J. Alero Thomas, and Theresa H. Ward[2]

Immunology Unit, Department of Infectious and Tropical Diseases, London School of Hygiene and Tropical Medicine, London, United Kingdom

RECEIVED DECEMBER 30, 2008; REVISED SEPTEMBER 15, 2009; ACCEPTED OCTOBER 5, 2009. DOI: 10.1189/jlb.1208774

ABSTRACT

The differentiation of B cells into Ig-secreting plasma cells requires the expansion of secretory organelles to cope with the increased cargo load. To evaluate the timeline of this process, we have quantitated the kinetics of secretory organelle expansion relative to Ig secretion and examined regulatory components of secretory transport following in vitro activation of human B lymphocytes. Unstimulated B cells contain minimal endomembranes. After activation, ER membrane induction appears as tightly packed spherical structures of 0.5–1 μm diameter concentrated in a juxtanuclear position. When the cells differentiate into plasmablasts, there is dramatic cell-size increase, but the ER remains concentrated close to the nucleus and only later fills the entire cell. In sharp contrast, previous studies in other cell types have found that the ER expands in synchrony with increasing cell size during interphase, by extension of ER tubules under the PM. In this study, the Golgi remains consistently as a single juxtanuclear structure but linearly expands sixfold in volume during B cell activation. Furthermore, following active cell proliferation, ER exit sites proliferate rapidly, increasing almost fourfold in number, in parallel with a sharp increase in Ig secretion. These findings demonstrate that the control of organelle biogenesis and expansion in primary human B cells are differentially regulated by cargo flux caused by Ig synthesis. *J. Leukoc. Biol.* 87: 245–255; 2010.

Introduction

Plasma cells are terminally differentiated key mediators of the humoral immune response, formed when resting B lymphocytes are activated by antigen. B cell morphogenesis into large antibody-secreting plasma cells demands total commitment to protein synthesis through the expansion of the secretory pathway to form a highly developed endomembrane transport network.

The secretory pathway is ubiquitous to all cells and essential for the export of proteins. Resting B cells characteristically contain minimal cytoplasm, rudimentary ER, and express only surface Ig. Following antigen stimulation, surface Ig is downregulated, and the cell starts to secrete soluble Ig, and by terminal plasma cell stage, copious secretion rates of up to 3000 antibody molecules/s are achieved [1]. To accommodate this secretory load, plasma cells form an elaborate ER network, containing a host of chaperones required for correct folding and assembly of Ig molecules. From the ER, assembled proteins are recruited to ER exit sites—small, specialized domains along the length of the ER—and are packaged by the sequential action of coat proteins (COPII then COPI) into carriers destined for the Golgi apparatus [2, 3]. In the Golgi, Ig molecules undergo further glycosylation before transport to the PM.

Differentiation of lymphocytes is accompanied by progressive changes in the cell-surface protein repertoire. During plasma cell generation, mature, naïve B cells ($CD19^+$, $CD20^+$, $CD38^{\pm}$, $CD138^-$) convert to a characteristic plasma cell phenotype ($CD19^{\pm}$, $CD20^-$, $CD38^{hi}$, $CD138^+$) [4]. Recent molecular studies have shed light on the interplay among transcription factors, including Pax5, XBP-1, while Blimp1, underlying these phenotypic changes in controlling cellular differentiation [5, 6]. Pax5 inhibits plasmacytic differentiation through transcriptional repression of several B cell differentiation factors, including XBP-1 and Blimp1 [5], which are key factors essential for plasma cell formation, while Blimp1 acts as a transcriptional activator necessary for high-level Ig synthesis and a repressor of Pax5 [6]. XBP-1 regulates plasma cell differentiation [7] and is one of the three transducers of the UPR in B cells [8]. The UPR is a cellular response

Abbreviations: 3D=three-dimensional, AP=antisense primer, ATF6=activating transcription factor 6, Blimp1=B lymphocyte-induced maturation protein-1, COPI/II=coat protein complex I/II, DAPI=4′,6-diamidino-2-phenylindole, ER=endoplasmic reticulum, ERGIC-53=ER-Golgi intermediate compartment 53, IRF-4=IFN-regulatory factor 4, IRE1=inositol-requiring protein 1, LSHTM=London School of Hygiene & Tropical Medicine, MRC=Medical Research Council, Pax5=paired box gene 5, PFA=paraformaldehyde, PM=plasma membrane, PWM=pokeweed mitogen, qRT-PCR=quantitative RT-PCR, RER=rough ER, SAC=*Staphylococcus aureus* Cowan strain protein A, SP=sense primer, TBP=TATA box-binding protein, TEM=transmission electron microscopy, UPR=unfolded protein response, XBP-1=X box-binding protein 1

The online version of this paper, found at www.jleukbio.org, includes supplemental information.

1. Current address: Biopharm R&D, Domantis Limited, Cambridge CB4 0WG, UK.

2. Correspondence: Immunology Unit, Dept. of Infectious and Tropical Diseases, London School of Hygiene and Tropical Medicine, Keppel St., London WC1E 7HT, UK. E-mail: theresa.ward@lshtm.ac.uk

to excessive amounts of unfolded proteins, which place high amounts of stress on the ER. In the context of B cell differentiation, UPR signaling, activated during plasma cell differentiation, results in increased transcription of ER chaperones and other components that aid Ig folding and secretion [9] and, potentially, plays a key role in the final expansion of membranes that ultimately lead to cell death.

A number of cytokine and mitogen-based assays have been developed to monitor primary human B cell differentiation in vitro [10–12]. In this study, a multivalent stimulation with pokeweed mitogen, SAC, and CpG DNA, originally described in ref. [13], was found to facilitate most effectively full differentiation of primary circulating human B cells to plasma cells within a timeframe that could be followed by microscopy. Here, this in vitro activation assay has been used in conjunction with quantitative light and electron microscopy techniques to profile changes in the ER, together with the Golgi and ER exit sites, throughout the B cell differentiation process. The findings offer important insights into the coordination of organelle dynamics in the course of Ig secretion in early effector B cells and antibody-producing plasma cells.

MATERIALS AND METHODS

Chemicals and antibodies

All chemicals were from Sigma-Aldrich (Poole, Dorset, UK) unless otherwise stated. Antibodies used in this study are described in Supplemental Table 1.

Isolation and stimulation of peripheral human B cells

PBMC were isolated by density centrifugation over Ficoll Histopaque-1077 from fresh, anonymous, human donor blood obtained under ethical consent from a pool of healthy volunteers at LSHTM. $CD20^+$ B cells were positively selected using MACS Microbeads (Miltenyi Biotec, Surrey, UK), according to the manufacturer's instructions, and counted on a Neubauer hemocytometer. Typically, $1–3 \times 10^6$ $CD20^+$ B cells were isolated from a single donation of 50 ml peripheral blood, and three to five donors were used for each experiment. Immediately upon isolation, B cells were diluted to 5×10^5 cells/ml in B cell medium (HEPES-buffered RPMI, 10% FCS, 2 mM glutamine, 0.1 mg/ml streptomycin, 100 U/ml penicillin), supplemented with the combined antigen mixture (hereafter, mitogenic antigen mixture) of 100 μg/ml SAC, 10 μg/ml PWM, and 1 ng/ml CpG2006 (Eurogentec Ltd., Romsey, UK) to induce differentiation [13], and incubated in a single pooled culture, unless otherwise indicated, at 37°C with 5% CO_2. Cells were analyzed by removal of an appropriate aliquot from the stimulated culture at the time-points indicated in the text—over a period of up to 7 days—and processed according to the experimental method.

Flow cytometry

B cells (1×10^6) were washed with FACS buffer (PBS, 1% FCS, 0.1% NaN_3), stained with directly conjugated cell-surface marker antibodies (Supplemental Table 1) or their isotype controls, for 30 min at room temperature, washed in FACS buffer, then fixed in 4% PFA in FACS buffer for 15 min at room temperature, and washed again. Acquisition was performed on a FACSCalibur (BD Biosciences, Oxford, UK) and data analyzed using FlowJo software (Version 8.1.1, Tree Star, Ashland, OR, USA).

Ig ELISA

$CD20^+$ B cells were stimulated with mitogenic antigen mixture, and supernatants were collected at daily intervals. Duplicate supernatants were assayed for secreted IgM levels by sandwich ELISA. Briefly, Maxisorp Immulon 4HBX plates (Thermo Life Sciences, Basingstoke, UK) were coated with rabbit anti-human IgM and incubated with serially diluted (1:1–1:500) B cell supernatants for 2 h at 37°C. Plates were washed in PBS/0.05% Tween 20 and incubated with HRP-conjugated anti-IgM antibody for 1 h. Plates were developed with SureBlue substrate solution (Insight Biotechnologies, Middlesex, UK), terminated with 1 M H_2SO_4, and the absorbance read at 492 nm in Dynex MRX plate reader (Worthing, UK). Standard curves were created from readings of serially diluted, purified human IgM (1–125 ng/ml). Secreted IgG levels were measured using the human IgG ELISA quantitation kit (Bethyl Laboratories, Cambridge Bioscience, UK), according to the manufacturer's protocol.

Proliferation assay

Purified $CD20^+$ B cells were incubated in 96-well round-bottomed microtiter plates at 1×10^5 cells/well in 200 μl B cell medium in the absence (unstimulated) or presence of mitogenic antigen mixture (stimulated). For the last 16 h of the incubation time indicated, 0.5 μCi methyl-[^{3}H]-thymidine (TRK120, GE Healthcare, Piscataway, NJ, USA) was added. DNA from the cell cultures was harvested onto filter papers using a Dymax washer and harvester (Tomtec, Hamden, CT, USA). [^{3}H]-Thymidine incorporation was determined using a Wallac Trilux™ 1450 MicroBeta liquid scintillation counter (Perkin Elmer, Wellesley, MA, USA). Results shown are mean cpm ± SD of triplicate cultures from one representative experiment.

Immunofluorescence and live cell stains

B cells were adhered to poly-L-lysine-coated #1 coverslips for 60 min, fixed in 2% PFA in PBS at room temperature (anti-giantin and B cell surface markers) or methanol at –20°C for 10 min (anti-Sec24C). Cells were incubated with antibody diluted in PBS containing 5% FCS and 0.1% saponin for 1 h at room temperature with washes in 5% FCS/PBS. Cells were mounted in Fluoromount G (Cambridge Biosciences, UK) with DAPI to label nuclei. DRAQ5™ (Biostatus Ltd., Leics, UK) and calcein (Live/Dead® viability/cytotoxicity kit, Molecular Probes, Invitrogen, Paisley, UK), which are vital dyes for nuclei and live cells, respectively, were used per the manufacturers' instructions, and live, stained cells were imaged in Nunc Lab-Tek™ eight-chambered coverglasses (VWR International, UK) with the microscope stage heated to 37°C. Cells were stained with 0.1 μM ER-Tracker™ Blue-White DPX in PBS (Molecular Probes) at 37°C for 20–30 min, washed in PBS, then stained, with antibodies to B cell phenotypic markers for 15 min in B cell media at 37°C, and washed again. Cell suspension was applied to an imaging chamber described in ref. [14], sealed with a poly-L-lysine-coated coverslip, inverted to enable cells to stick to poly-L-lysine, and imaged with the microscope stage heated to 37°C.

Confocal microscopy

Fluorescence images were obtained with a Zeiss LSM 510 confocal microscope using 405 nm, 488 nm, 543 nm, and 633 nm laser lines for the appropriate dyes. Live cells were imaged at 37°C on the stage with a 100× 1.4 numerical aperture objective set at a pinhole diameter equivalent to 1–1.3 Airey units. Images were analyzed using the Zeiss LSM software or Volocity 4.2 (Improvision, UK).

To quantitate ER exit site distribution, z-stacks of cells labeled for Sec24C and DAPI were acquired by confocal microscopy and imported into Volocity. ER exit sites were labeled manually and counted for each cell in a 3D projection for each day during the time course. Four independent COPII labeling experiments were used. Golgi morphology was assessed by 3D confocal imaging of differentiating B cells labeled by immunofluorescence of the Golgi marker giantin. z-stacks were imported into Volocity and used for volumetric analysis. Seven independent Golgi-labeling experiments were used for quantification.

Electron microscopy

B cells (1×10^7) were fixed in 2.5% glutaraldehyde/2% PFA/0.1 M Na cacodylate, pH 7.4, and washed in 1% PFA/0.1 M Na cacodylate. The cells were post-

fixed in osmium tetroxide, embedded in agar, dehydrated in methanol, and embedded in TAAB hard resin (TAAB, Berks, UK). Ultrathin sections were cut on a Leica Ultracut R microtome, stained with Reynolds lead citrate, and observed in a Jeol JEM 1200EX II transmission electron microscope.

TEM images were imported into the imaging software Adobe Photoshop®. Using a graphics pen, the rough ER membrane, nucleus, and total cell area were overlaid manually as separate components. The masked images were calibrated and quantified in Volocity (Supplemental Fig. 1). The nuclear envelope was not included in total ER measurements, as for the purposes of ER expansion, the nucleus does not vary greatly in size during differentiation.

Real-time qRT-PCR to determine mRNA expression level

Standards for each gene of interest were generated by conventional PCR from PBMC-derived cDNA, followed by purification using the QIAquick PCR purification kit (Qiagen, Valencia, CA, USA) and quantified using the PicoGreen® method (Invitrogen). Copy numbers were calculated based on the fragment length, and standards were used in subsequent assays to generate standard curves ranging from 10^6 copies to 10 copies/reaction. RNA was prepared from stimulated B cells using the RNeasy mini kit (Qiagen) according to the manufacturer's instructions, and 50 ng total RNA was reverse-transcribed in duplicate using an oligo dT primer and Superscript II enzyme (Invitrogen). The 20-μl reaction mix was diluted to 100 μl with water. The expression levels of the indicated genes were measured by real-time qRT-PCR using SYBR® Green (Applied Biosystems, Foster City, CA, USA) incorporation in an ABI Prism 7000 sequence detection system (Applied Biosystems) by reference to the standard curve for each gene. Results are shown normalized to TBP mRNA copy number, as this gene was found to be the most stably expressed housekeeping gene in stimulated B cells using the geNorm application (S. J. Kirk and J. M. Cliff, unpublished observations; ref. [15]). Each reaction was performed with 5 μl cDNA, 12.5 μl SYBR Green Mastermix, 1 μl each primer (final concentration, 400 nM), and 5.5 μl water. PCR conditions were 10 min 95°C denaturation step, followed by 40 cycles of 95°C:15 s/60°C:1 min. At the end of all of the cycles, a dissociation analysis was performed to ensure the presence of only one specific PCR product.

Primer sequences were: ERGIC-53 SP: GACATCAAAGAGCACCTGCACA, AP: ACAAACATGATGGAAATGGTGGT; Blimp1 SP: CGGGAGAAAAGCCACATGAA, AP: TCCAGAATGGAGTCGCAGGT; IRE1 SP: TCTCCTCCGAGCCATGAGAA, AP: GGGGGAAGCGAGATGTGAAG; IRF-4 SP: CCTGCAAGCTCTTTGACACACA, AP: TGGAAACTCCTCTCCAAAGCA; Sec24C SP: CCAGAGCCTTTTCAGCGTCTC, AP: GCCTCGAACCTTCTTGGACA; Sec31A SP: GCTGCCTTTCTTCAGCAACAG, AP: TCGAGTTTCAATGCTCCTTGC; XBPI-S SP: AGAGGAGGCGGAAGCCAAG, AP: GTCCAGAATGCCCAACAGGA; XBPI-U SP: AGAGGAGGCGGAAGCCAAG, AP: TCTGGAGGGGTGACAACTGG.

Immunoblotting

At the given time-points, 3×10^6 B cells were lysed in 200 μl sample buffer (10% glycerol, 2% SDS, 250 mM Tris, pH 6.8, 0.01% bromophenol blue, 20 mM DTT). Extract equivalent to 3×10^5 cells was resolved by reducing SDS-PAGE as described previously [14]. Western blot images were acquired by detection of antibody-protein complexes using ECL (GE Healthcare).

RESULTS

In vitro B cell stimulation assay leads to terminal plasma cell-like differentiation

To test whether the mixed mitogenic antigen-stimulation protocol was able to induce differentiation of primary B cells to terminal stage plasma cells, cell-surface phenotype, morphology, and Ig secretion were analyzed over 7 days. To monitor B cell surface-antigen expression, purified $CD20^+$ peripheral primary human B cells were cultured with mitogenic antigen mixture for 7 days, and aliquots were removed for phenotypic analysis (CD19, CD38, and CD138) on Days 0 and 7 (**Fig. 1A**). CD19 was expressed on resting $CD20^+$ B cells (Day 0) and reduced to low levels by Day 7, indicating down-regulation of expression over time. By contrast, CD38 expression was up-regulated, and cells at Day 7 had high levels of surface expression compared with unstimulated cells. CD138 was not expressed at early time-points but was found on up to 30% of cells following 6–7 days' stimulation. As a result of rapid death of terminally differentiated cells, this number may be lower than the total percentage that becomes $CD138^+$. Comparative flow cytometric analysis similarly showed that between Days 0 and 7, $CD19^+$ cell numbers decreased, and $CD38^+$ cell numbers increased, with 68% B cells at Day 7 found to be $CD38^{hi}$ (Supplemental Fig. 2). Forward- and side-scatter analysis showed that with increase in CD38 expression, cells exhibited increased size and granularity.

As B cell activation leads to clonal expansion in vivo, it was necessary to test whether the mitogenic antigen mixture was able to induce cell proliferation. Incorporation of [^{3}H]-thymidine is a measure of DNA synthesis, which can be used as an indicator of cell proliferation. [^{3}H]-Thymidine uptake over the 7-day assay period was assessed (Fig. 1B). Upon stimulation, B cells underwent cell division rapidly, with rate of [^{3}H]-thymidine uptake peaking at Day 2, after which, cells terminally differentiated as nonproliferating plasma cells, as indicated by diminished [^{3}H]-thymidine uptake. Analysis of cell viability over the time course demonstrated an increase in the proportion of dead cells only at Days 6 and 7 (data not shown), which indicated that the decline in proliferation was not linked to cell death.

The effects of the mitogenic antigen mixture on Ig production were investigated (Fig. 1, C and D) by daily sampling of supernatants from cultures of stimulated B cells. Sandwich ELISAs revealed induction of IgM from Days 3 to 4 with maximum levels detected by Day 7 (Fig. 1C). IgG levels were found to increase rapidly from Day 4, reaching a plateau by Day 6 (Fig. 1D). This indicated that Ig secretion induction occurred following the proliferative phase.

Using calcein and DRAQ5™, freshly isolated $CD20^+$ B cells were found to have a uniform appearance, 5 μm in diameter, an almost spherical shape, few membranous extensions, and sparse cytosol around the nucleus (Fig. 1E). Cells at Day 7 were smoother, more ovoid, with the nucleus pushed to one side by the volume of cytosol, in a manner characteristic of plasma cells.

These morphologic changes, together with evidence of induction and increasing secretion of Ig molecules, demonstrated clearly that the mixed mitogenic antigen method of stimulation was driving naïve, resting B cells to terminal plasma cell differentiation.

Expansion of the internal membranes precedes up-regulation of Ig secretion

ER membrane configuration was investigated by looking at the cell ultrastructure at different stages of plasma cell biogenesis (**Fig. 2A**). At Day 0, most cell profiles exhibited a single layer of ER around the nucleus, corresponding to the nuclear envelope, and, in most cases, no peripheral strands of ER were observed in the cytosol, correlating with the

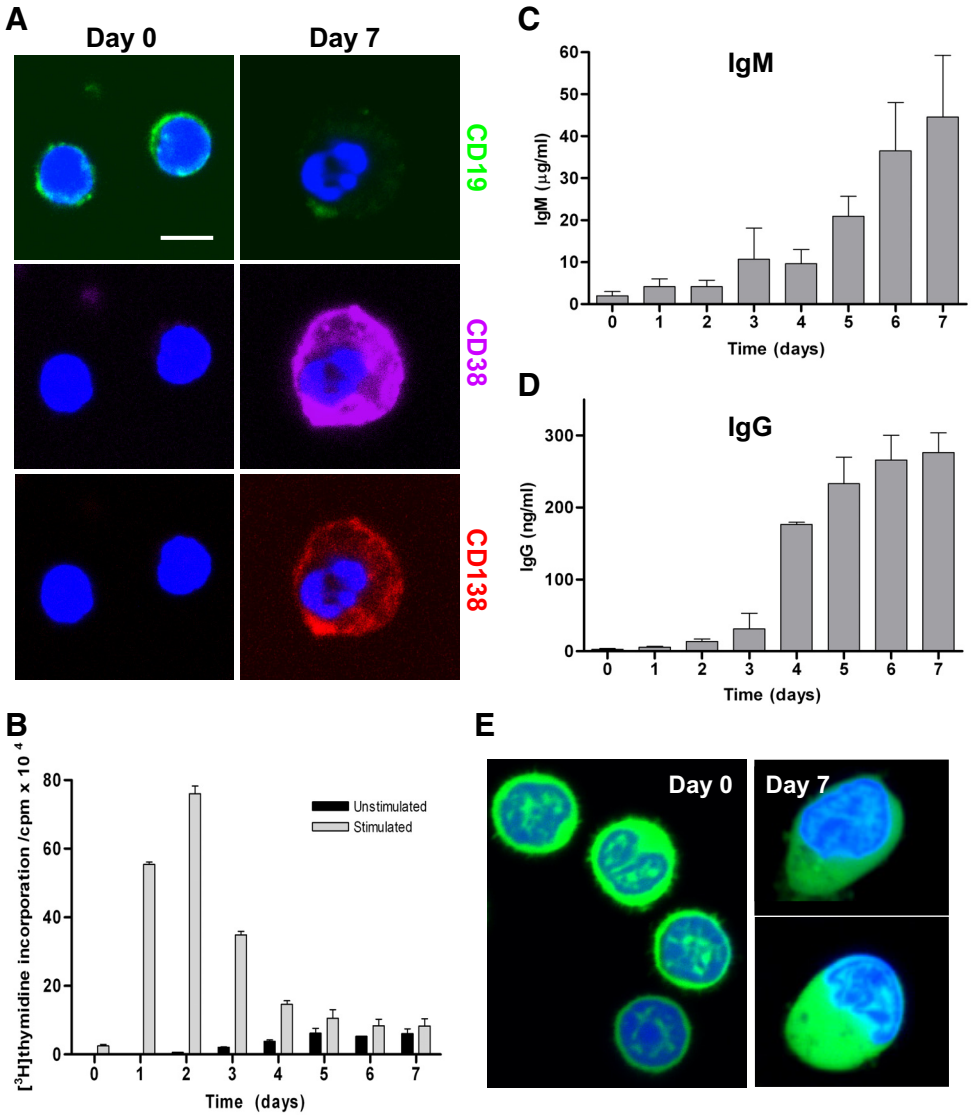

Figure 1. The combination of CpG, SAC, and PWM induces terminal differentiation of peripheral blood B cells. After isolation, primary human B cells were stimulated with mitogenic antigen mixture for a period of 7 days. (A) Unstimulated B cells (Day 0) and plasma cells (Day 7) were stained for the expression of B cell markers CD19 (green) and CD38 (purple) and plasma cell marker CD138 (red), with DAPI (blue) to label nuclei, and visualized by confocal microscopy. Original bar, 5 μm. (B) Equal numbers of cells, stimulated by antigen mixture, were pulsed with [^{3}H]-thymidine and then harvested at the indicated times (from stimulation start-point). Cell proliferation was determined by [^{3}H]-thymidine incorporation as a measure of DNA synthesis, represented as cpm. Each experiment value is a mean of triplicates ± SD from one representative experiment. To investigate the levels of secreted Ig, supernatants were harvested from the stimulated B cells at daily intervals. The presence of IgM (C) or IgG (D) was detected by sandwich ELISA. Each value represents the mean ± SD from duplicate assays of four independent experiments. (E) To examine cell morphology, purified B cells were labeled with calcein (green) and DRAQ5™ (blue) to label DNA and visualized by confocal microscopy. Examples of cells from Day 0 (unstimulated) and Day 7 are shown.

compact size of the nonactivated B cells. By Day 3, proliferation of the ER was clear, and at Day 7, there was a highly compacted ER ultrastructure, densely coated in ribosomes, indicating RER proliferation (Fig. 2, A and B). In some cells, this ER structure was distorted, showing greatly dilated RER cisternae and highly crystalline proteinaceous lumenal content (Fig. 2B). Fine strands were sometimes visible in the distended ER lumen (Fig. 2B). Up-regulation of the peripheral ER was quantitated by manual overlay of the electron micrographs (Fig. 2C and Supplemental Fig. 1). Measurement of total peripheral RER profile and cell cytosol revealed that the ER:cytosol ratio expanded >140-fold between Days 0 and 3 ($P<0.01$; Student's t-test) and doubles again between Days 3 and 7 ($P<0.01$). Interestingly, ER expansion seemed to occur within specific areas of the cell. At Day 3, RER was up-regulated greatly, but there were regions of cytosol lacking ER (Fig. 2A and Supplemental Fig. 1). In comparison, the ER in Day 7 cells extended throughout the cytosol, with exclusion zones only for other organelles such as mitochondria (Fig. 2A). This was verified when ER was quantified (Fig. 2C), where the further doubling of the ER:cytosol ratio reflected increased density of ER membranes throughout the cytosol. In contrast, mitochondrial numbers were found to increase significantly between Days 0 and 3, but no further increase was seen between Days 3 and 7 (Supplemental Fig. 3).

Induction of UPR has been implicated in alteration of ER dimensions [16]. As B cell differentiation uses UPR pathways, ER dimensions were investigated in this system. Tracing of tubule diameters showed a clear change in lumenal volume during differentiation (**Fig. 3A**). Notably, there was no discernible difference between peripheral ER and the nuclear envelope in naïve B cells (Day 0; Fig. 3, A and B). By contrast, in plasma cells, the nuclear envelope maintained its original dimensions, and the peripheral ER exhibited marked lumenal enlargement (Day 7; Fig. 3, A and B). Measurements of the lumen diameter clearly demonstrated shifting ER lumenal profiles among different time-points (Fig. 3C), changing from 20.5 nm ± 9.2 in

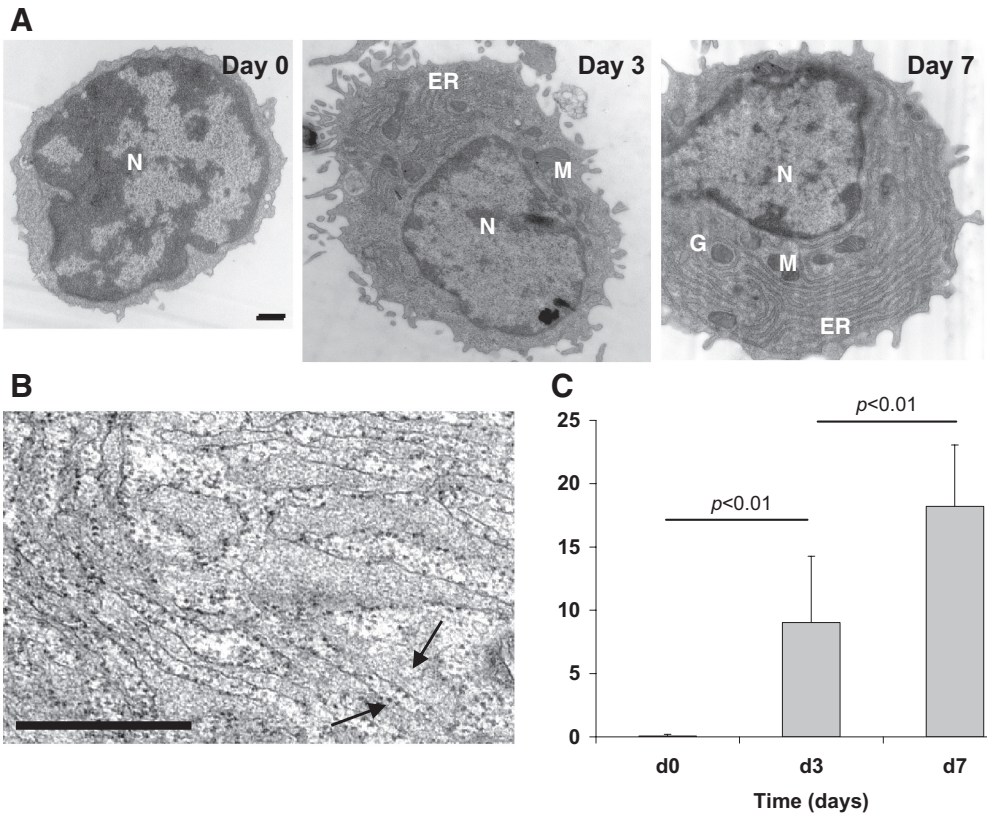

Figure 2. ER membranes are up-regulated during B cell differentiation. Purified human CD20$^+$ B cells were stimulated with mitogenic antigen mixture. (A) Electron micrographs of unstimulated B cells (Day 0) or B cells stimulated for 3 and 7 days. Representative cells are shown. N, Nucleus; M, mitochondrion; G, Golgi. Original bar, 500 nm. (B) Enlargement of electron micrograph of plasma cell RER (Day 7) to show proteinaceous lumenal content. Arrows point to strands inside ER lumen. (C) TEM images of cells were used to quantify the increase in RER membranes through B cell differentiation. Masks were created of nuclei, ER membranes, and total cell area in Adobe Photoshop and then calibrated and quantitated in Volocity, and ER as a proportion of cytosol was calculated (see Supplemental Fig. 1). Data are presented as mean ± SD. Statistical significance is indicated.

unstimulated cells to 41.3 nm ± 27.0 at Day 3 and 68.3 nm ± 34.4 at Day 7, which was statistically significant ($P<10^{-5}$ in all combinations). Variable ER morphology found in plasma cells, with some thinner tubules and other greatly expanded sections, was reflected in the increased SD. ER tubules measuring >50 nm were not found in undifferentiated cells (Fig. 3D), whereas the frequency of dilated ER tubules had increased significantly by Day 3, and by Day 7, 60% of ER measurements exhibited distension >50 nm.

CD20$^+$ cells were stained with ER-Tracker to examine ER membrane induction in live cells at early time-points during B cell differentiation. In unstimulated cells, the ER labeled as a thin line of fluorescence, around the nucleus closely aligned to the PM and some concentrated membranes located in nuclear invaginations. This indicated that the majority of ER at this stage was confined to the nuclear envelope with minimal amounts in the periphery (**Fig. 4, A–C**). After stimulation (Day 1), cells showed morphological variation, with the nuclei often appearing distended, and the peripheral ER began to proliferate but remained closely underlying the PM (Fig. 4, D–F). The ER proliferated as distinct fluorescent puncta polarized to one side of the nucleus (Fig. 4E and Supplemental Movie 1). On Day 2, cell size and ER membranes were visibly expanded (Fig. 4, G–I), the latter appearing as tightly packed spherical structures (0.5–1 μm diameter) associated with the nucleus. Spaces lacking ER underneath the PM (labeled for surface antigen) were apparent (Fig. 4, G, I, J, L). Areas in the cytosol without ER were similarly found at EM level (Supplemental Fig. 1, Day 3). As cells continued to differentiate, the tightly packed ER spheres appeared to expand to fill the cytosol, and ring-like structures were seen in many cells (Fig. 4, N, O, Q). This data suggest that ER expansion is not synchronized to cell size/shape in differentiating B cells and that ER biogenesis may occur by accumulation of membranes close to the nucleus before expansion through the cell.

With respect to changes in the Golgi apparatus during plasma cell biogenesis, from Day 0 to Day 7, Golgi membranes changed from a small, compact 1 μm juxtanuclear structure to an expanded, lobed structure (**Fig. 5A**), comparable with enlarged Golgi found in CD138$^+$ cells isolated directly from peripheral blood (data not shown). Quantitation studies showed that the membranes increased linearly in size by 6.5-fold throughout differentiation (Fig. 5C). At an ultrastructural level, tightly packed cisternae apparent at Day 0 (Fig. 5B) became dilated at Day 7 (plasma cell stage) with pronounced accumulation of vesicular membranes in the vicinity of the Golgi cisternae.

To investigate changes in the ER exit sites, isolated CD20$^+$ B cells were stimulated, fixed at indicated time intervals, and stained for Sec24C (Fig. 5E), a component of the COPII coat that selectively associates with ER exit sites [2, 3]. At Day 0, ER exit sites were sparsely, but evenly, distributed around the nuclear envelope in sharp punctate structures. At early time-points (Days 1–3) following stimulation, these punctate structures persisted, and at later time-points (Days 5–7), the number of ER exit sites visibly increased and was found eccentrically distributed to one side of the nucleus. Quantitation of ER exit sites (Fig. 5D) demonstrated a marked increase between Days 3 and 7, paralleling the onset and up-regulation of Ig synthesis.

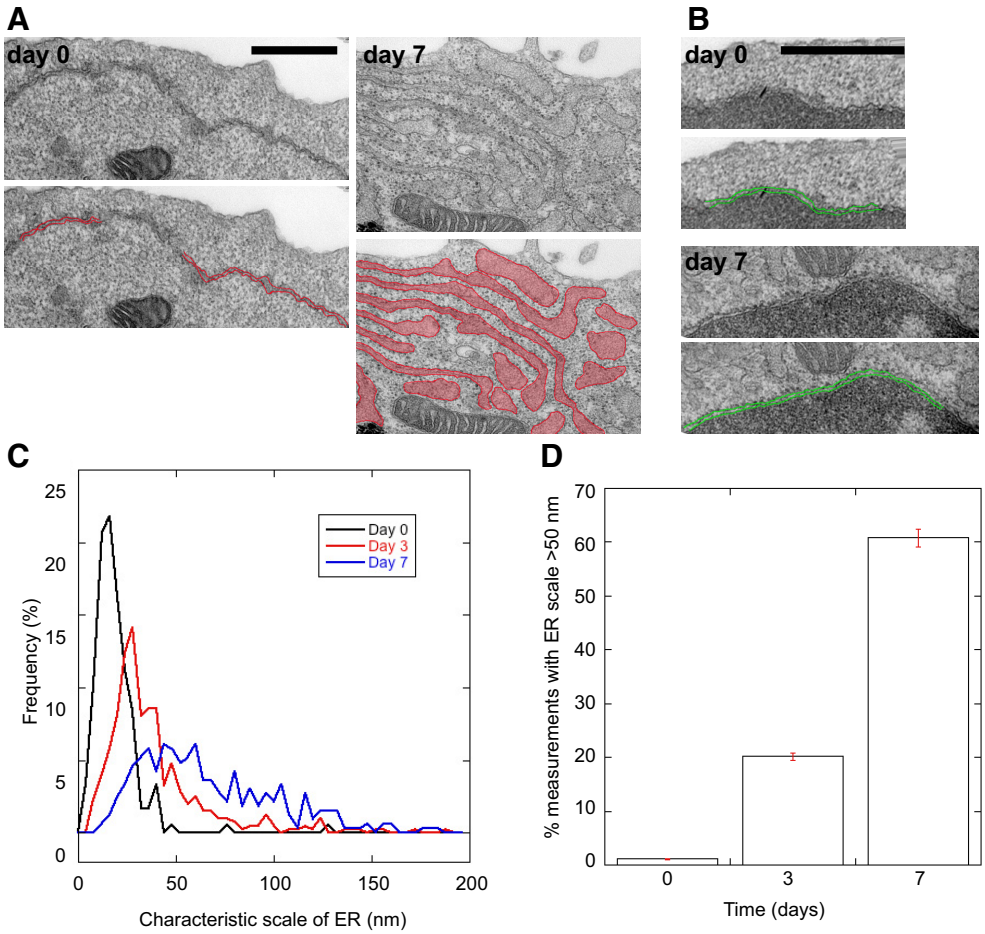

Figure 3. ER dilation during B cell differentiation. Electron micrographs show peripheral ER (A) and the nuclear envelope (B) at Days 0 and 7. Each image shows a representative example of a section of peripheral or nuclear envelope ER, alongside an image overlaid to delineate the membrane paths. Peripheral ER is represented in red and nuclear envelope in green. Images were acquired at ×40,000 original magnification. Original bars, 500 nm. (C) TEM images were imported into Volocity, and measurements of distance between ER membranes were taken at regular intervals. Data are presented as a histogram of frequency of measured distances at the different time-points. (D) Graph showing frequency of measurements >50 nm at the different time-points ± SD. 50 nm was chosen as a gating value based on 99% of Day 0 measurements falling below this point.

ER exit site components are up-regulated during differentiation

Investigation of components involved in up-regulation of endomembranes and Ig secretion showed that key transcription factor mRNA levels are differentially regulated during B cell differentiation (**Fig. 6A**). Pax5, which is a transcriptional repressor of several B cell differentiation factors [5], was repressed from the outset, whereas mRNA encoding late B cell regulators Blimp1 and IRF-4 [17, 18] was induced, with expression peaking on Days 4–5. Interestingly, IRF-4 additionally showed an early induction peak on Day 1, a pattern not found in the other B cell transcription factors investigated, indicating a potential early role for IRF-4 in B cell activation.

XBP-1, a regulator of the UPR that is essential for plasma cell development, was also up-regulated in spliced and unspliced forms. Splicing of XBP-1 mRNA is dependent on the activity of IRE1 [8], an ER-resident stress-activated endonuclease. mRNA encoding IRE1 was up-regulated at Day 4, correlating with the increased levels of the spliced XBP-1 transcript. ERGIC-53 has been linked to the UPR [19] and has been implicated in Ig sorting and exit from the ER [20]. Concomitant with up-regulated transcription factors, ERGIC-53 expression levels peaked at Day 5, with an almost tenfold increase in expression, indicating that ERGIC-53 expression is correlated to Ig output.

The COPII coat regulates exit from the ER, and its component proteins must be up-regulated for proliferation of ER exit sites to occur. We found that expression of COPII components Sec24C and Sec31A was up-regulated 2.5-fold with a peak at Days 4–5 as for up-regulated B cell differentiation factors. Significantly, Sec24C showed an elevated level of expression at Day 1, a pattern also seen in IRF-4 expression but not in other transcription factors (Fig. 6A).

To validate that increase in mRNA expression reflects up-regulation of the encoded protein, whole cell extracts were immunoblotted for secretory pathway components. A sharp increase was found in components involved in protein folding in the ER (calreticulin), in regulation of ER exit (Sec24C), and in cargo sorting (ERGIC-53) by Day 3 with further increases by Day 7 (Fig. 6B), consistent with the mRNA expression pattern. Therefore, up-regulation of regulatory proteins required for assembly and transport of Ig molecules through the secretory pathway mirrors the onset of Ig synthesis and subsequent high levels of secretion.

DISCUSSION

Historically, studies examining secretory components in differentiating B cells have used electron microscopy predominantly to

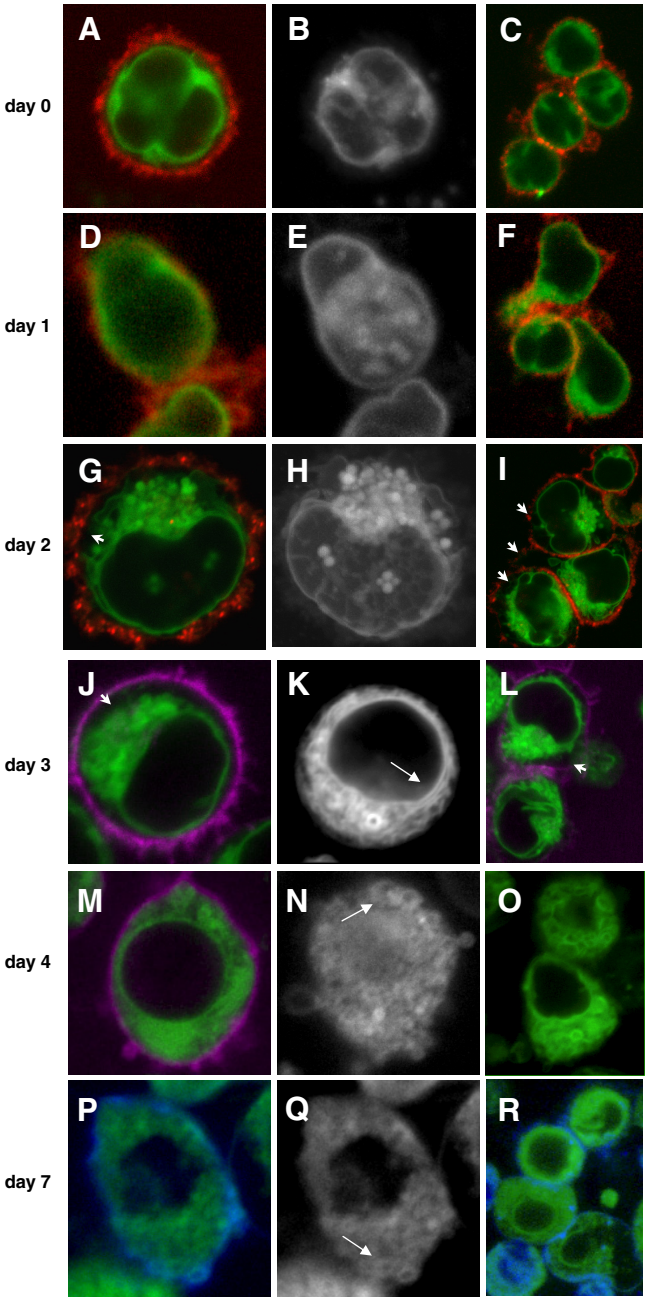

Figure 4. Gross ER morphology alters dramatically during differentiation. At the indicated time-points, live cells were costained with Blue-White ER-Tracker (green) and B cell markers, CD19-FITC (red), CD38-Alexa647 (purple), and CD138-PE (blue). Cells in suspension were mounted on an imaging chamber and visualized by confocal microscopy. Unstimulated (Day 0, A–C), Day 1 (D–F), Day 2 (G–I), Day 3 (J–L), Day 4 (M–O), and Day 7 cells (P–R) are shown with a representative surface marker. For each time-point, a cell cross-section (A, D, G, J, M, P) and a group of cells (C, F, I, L, O, R) at lower magnification are shown to demonstrate morphological similarity. (B, E, H) Projected Z-series of the cross-section panels to show total cell ER. (K, N, Q) Single-cell sections in grayscale to show more clearly expanded ER morphology. Arrows indicate individual ER tubules (K) or ring-like ER structures (N, Q); arrowheads indicate the gap between ER and PM (G, I, J, L). Cell-surface markers have been enhanced by modifying the image to a nonlinear look-up table using the γ-factor to enable visualization of the limiting PM.

demonstrate that plasma cells have extensive expansion of the RER, often found as tightly packed lamellae in parallel arrays [21, 22], in conjunction with expansion of the Golgi apparatus [23, 24]. To date, quantitative studies have used mouse splenocytes or stimulable murine cell lines [20, 23]. This study provides the first characterization of progressive secretory organelle biogenesis during primary human B cell differentiation.

Various combinations of cytokines and mitogens have been found to induce in vitro differentiation of primary human B cells [10–12]. In this study, a combination of three B cell mitogens, PWM, SAC, and CpG, used previously to proliferate a memory B cell population [13], was found to efficiently differentiate primary peripheral B cells into plasma cells with $CD38^{hi}$ and $CD138^{+}$ surface staining over a period of 7 days, a timeline analogous to LPS stimulation used in studies of mouse plasma cell formation (e.g., refs. [9, 25]). Using this method, B cells were activated swiftly, as indicated by the early induction of cell proliferation, which peaked at Day 2. Onset of IgM secretion was observed after the proliferative peak (Days 3–4), as the cells entered the lymphoblastoid stage of differentiation, and a steady increase was found for the duration of the assay with substantial IgM synthesis at late time-points. Similarly, onset of secretion of IgG occurred at Day 4 but plateaued at later time-points, indicating a decrease in the IgG secretion rate at the point at which $CD138^{+}$ cells were detected. It has been shown previously that the majority of IgG^{+} B cells after stimulation with CpG alone is derived from $CD27^{+}$ memory B cells, and naïve $CD27^{-}$ B cells are IgM^{+} [12]. Therefore, although high levels of IgG secretion by plasmablast cells derived from memory B cells are required in an immune response, the lower levels of IgG at late time-points seen here may reflect the behavior of long-lived $CD138^{+}$ IgG^{+} plasma cells in the bone marrow, where only low levels of secreted antibody would be required to maintain protective immunity [12]. Interestingly, no differences were observed in ER membrane up-regulation kinetics in $CD27^{+}$ and $CD27^{-}$ B cell subsets following stimulation with combined antigen mixture (data not shown).

Examination of ER biogenesis demonstrated an up-regulation of ER from essentially no peripheral ER in unstimulated cells to extensive stacked, ribosome-studded membranes over the course of activation to plasma cells, confirming the findings of others. A study quantitating ER up-regulation in the murine B cell line CH12 demonstrated a 3.7-fold increase in ER volume following LPS stimulation [23]. In contrast, our primary cells showed an effective 140-fold ER increase during the first 3 days of activation and a further doubling between Days 3 and 7. The discrepancy between these data is dependent on the ER baseline of the starting cell population, where CH12, the B cell line, already has a significant quantity of endomembranes prior to stimulation. In both cases, the plasma cell stage was found to contain similar relative amounts of RER. Significantly, by electron microscopy and live cell fluorescence, we found that early ER expansion does not extend throughout the cytosol, or in synchrony with cell expansion, but, by the plasma cell stage, the ER fills the cell. Using BCR-cross-linking to activate mouse splenic B cells, a previous study found a substantial increase in cytoplasm but little simultaneous up-regulation of ER membranes [26]. Although this stimulation assay may only recapitulate initial activation steps,

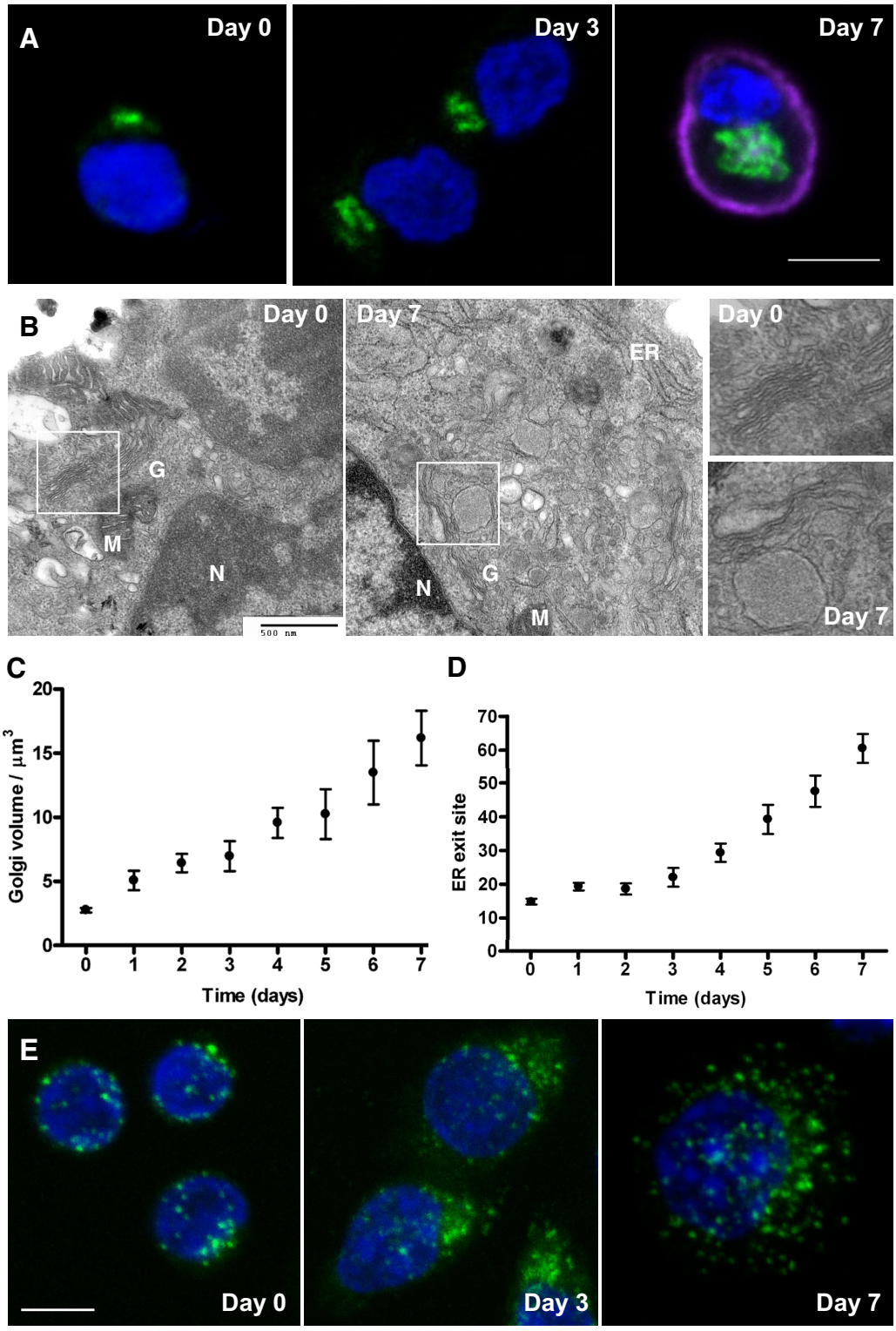

Figure 5. The Golgi apparatus and ER exit sites proliferate during B to plasma cell differentiation. Purified human CD20$^+$ B cells were stimulated with CpG, PWM, and SAC for the times indicated. (A) Cells were fixed and stained with r-giantin (green), CD38-Alexa647 (purple), and DAPI (blue) and viewed by confocal microscopy. Original bar, 5 μm. (B) Electron micrographs of the Golgi region in control, undifferentiated B cells (Day 0) and plasma cells (Day 7). Images acquired at ×40,000 original magnification. Original bar, 500 nm. Insets show magnification of the indicated areas. Fixed cells were stained for giantin (C) or Sec24C (D) at daily intervals, and serial Z-sections were acquired on the confocal microscope. Stacks were projected in Volocity. Golgi volume was quantitated as μm^3 (C), and ER exit sites were manually counted (D). Data are shown from at least three independent experiments. (E) Cells were fixed and stained with anti-Sec24C (green) and DAPI (blue) and viewed by confocal microscopy. Original bar, 5 μm.

as the cells are unable to terminally differentiate into plasma cells, this provides further evidence that differentiating B cells are driven to expand in size asynchronously to ER synthesis rather than ER expansion driving cell-size increase.

Additionally, ER proliferation in B cells appears to follow a different mechanism compared with most animal cell types. In previous studies of mammalian epithelial and fibroblast cell lines, cell growth occurs throughout interphase with simultaneous increase in organelle size/number [27–29]. ER proliferation in these cells occurs by extension along microtubules toward the cell periphery, and ER tubules underlie the leading edge of the PM [27, 30]. This process is dependent on micro-

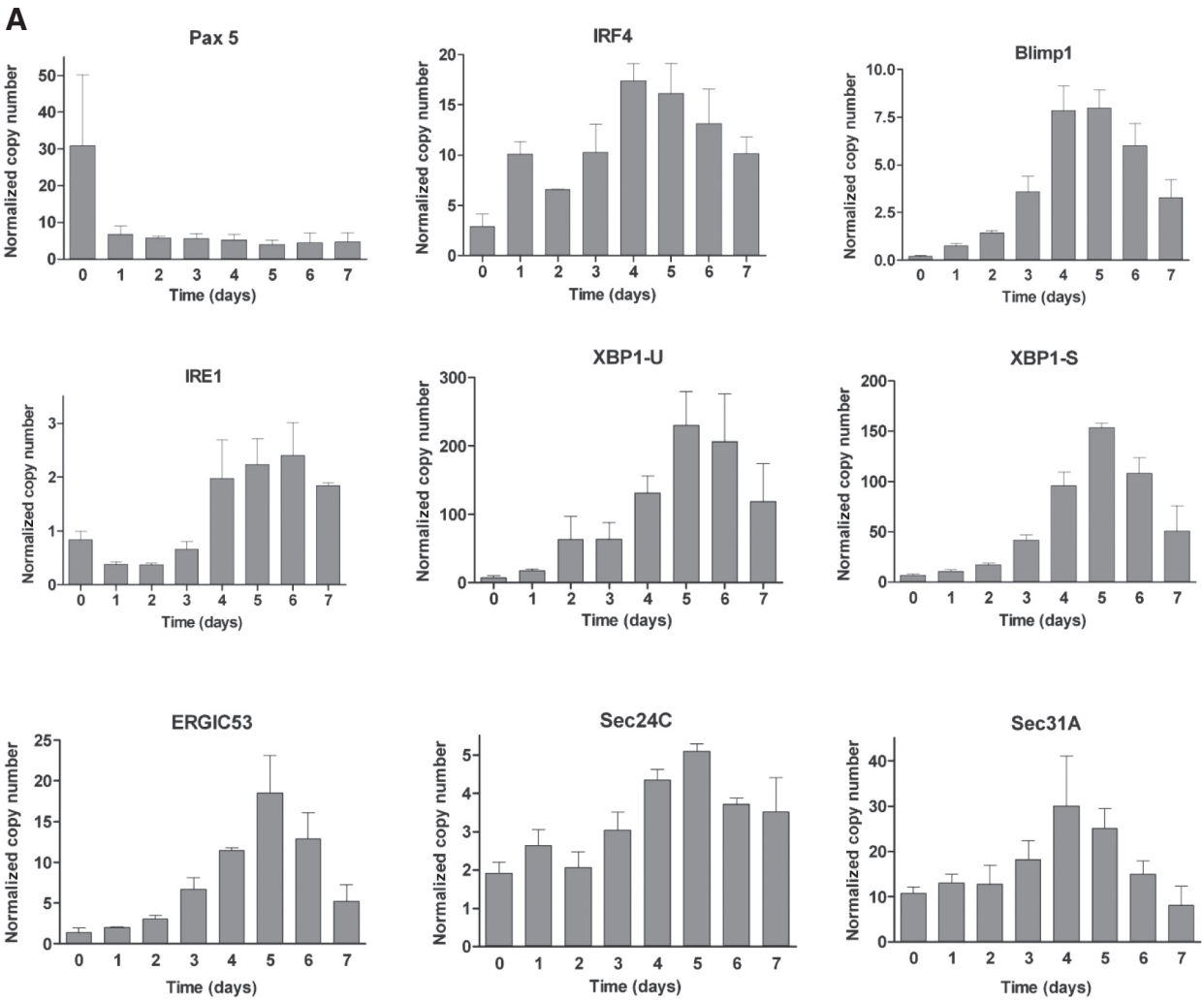

Figure 6. Regulatory molecules required for Ig egress from the ER are coordinately up-regulated during B cell differentiation. (A) Purified human $CD20^+$ B cells were activated with CpG, PWM, and SAC for 0–7 days, as indicated before RNA extraction and qRT-PCR. TBP was used to normalize expression levels. (B) Protein extracts from equal numbers of B cells stimulated over 7 days were analyzed by SDS-PAGE and Western blotting for components of the secretory machinery. Actin was included as a loading control.

tubule motors [31] and non-motor proteins such as cytoskeleton-linking membrane protein-63 [32]. Retraction of the ER from the cell periphery is usually associated with nocodazole treatment to depolarize microtubules, where the ER shrinks back to the nucleus and converts from tubules to sheets [27, 33]. Other studies in this laboratory (unpublished) have shown that the microtubule cytoskeleton remains intact in differentiating B cells. Thus, the finding of tight juxtanuclear ER membrane clusters in differentiating B cells reported here strongly suggests a novel route for ER biogenesis. How these ER structures interact with the cytoskeleton, and whether the activity of structural ER molecules usually associated with maintenance of extended ER tubules is altered, require further investigation.

The dramatic expansion of the ER during B cell differentiation is mirrored by a similarly expanded and well-developed Golgi. At the light level, the Golgi increases linearly in size throughout differentiation from a small 1-μm juxtanuclear structure to an en-

larged organelle of 4 μm diameter. The number of cisternae in each Golgi stack did not change, but in contrast to the uniform appearance of the stacks in undifferentiated cells, cisternae increased in diameter in plasma cells, indicating that the Golgi expands by increasing the number of stacks or by lengthening and distending its cisternae. The plasma cell Golgi exclusion zone (area that excludes RER and mitochondria) is greatly expanded and contains multiple vesicles in addition to the cisternae. In a previous study, quantitation of this area showed a 3.4-fold increase in volume in CH12 differentiation [23], whereas here Golgi volume showed a 6.0-fold increase. End-point Golgi volumes for each experiment were similar; therefore, the difference in Golgi growth may reflect differing starting baseline endomembranes, highlighting the difference between primary resting B cells used in the present study and B cell lines that are already partially differentiated [23]. In mammalian cell lines, Golgi volume increases in response to Golgi enzyme up-regulation but not in response to increased cargo flux [34]. Therefore, the gradual expansion of the Golgi apparatus from the onset of B cell differentiation may similarly reflect the up-regulation of Golgi-localized glycosylation enzymes prior to cargo transport initiation, i.e., before Ig induction.

The Golgi is maintained by a constant flux of proteins from the ER [35], and both can be viewed as one system maintained by a dynamic and constant cycling of proteins, lipids, and membranes. When this system is expanded during B cell differentiation, the balance of export and input to and from the ER must be adapted accordingly to allow expansion. This study provides the first evidence of ER exit site proliferation, concomitant with COPII up-regulation, through B cell differentiation. ER exit site biogenesis has been the focus of extensive research in other cell types, and the details of this process are not fully understood yet. Differentiating B cells provide an expanding system coupled to increasing cargo release and is thus a useful model to investigate ER exit-site regulation. In contrast to the effects on the Golgi, cargo-flux increase causes up-regulation of size and number of ER exit sites in adherent mammalian cell lines [34]. Although ER exit sites slowly increase in number in early B cell differentiation, which may reflect up-regulation of Golgi components, onset of Ig production and increasingly high levels of antibody secretion are paralleled by a rapid growth in ER exit-site numbers. It is also possible that expansion of the ER could drive a proportional increase in ER exit-site number. In interphase, ER exit-site numbers increase with cell size and by inference, proportional ER growth, such that immediately prior to prophase, cells have doubled the number of ER exit sites than at the start of interphase [28]. This ER exit-site biogenesis occurs in the absence of increased amounts of cargo in the cell. Therefore, it follows that during B cell differentiation, ER exit sites could proliferate in proportion to ER expansion and further, following onset of cargo induction. Furthermore, several of the COPII components have multiple isoforms. Those investigated in this study were found to be preferentially expressed in $CD19^+$ B lymphocytes and human B cell lines [36] but whether these are specifically required for Ig secretion remains to be elucidated.

Upon activation of B cells, mature B cell transcription factors (such as Pax5) are repressed, and repression of plasma cell transcription factors (such as Blimp1, XBP-1, and IRF-4) is removed [5, 6]. This transcriptional network is reflected here in the mRNA expression levels of these factors. XBP-1 is additionally regulated by UPR factors ATF6 and Ire1, which coordinate up-regulation of XBP-1 expression and splicing to form the more stable XBP-1(S), respectively. Expression of XBP-1(S) has been linked directly to ER expansion [25, 37] through up-regulation of ER proteins [25, 38] and phospholipid biosynthesis [39]. In mammalian cell lines, XBP-1(U) negatively regulates XBP-1(S) and is thought to be involved in recovery from the ER stress response [40]. As terminally differentiated plasma cells are unable to recover from the UPR, it is unclear whether XBP-1(U) has a direct role in differentiating B cells, if the protein is unstable in the plasma cell environment and is degraded rapidly, or whether accumulation of mRNA encoding XBP-1(U) is a by-product of overwhelming the splicing machinery.

UPR has been implicated in ER dilation as well as expansion in yeast cells under ER stress [16], increasing ER diameter 1.5-fold. In B cell differentiation, the UPR causes large distension of peripheral ER tubules (3.3-fold), and the nuclear envelope remains unchanged and is therefore unlikely to be a major site of Ig synthesis. We cannot discern whether the dilated peripheral ER is forming enlarged tubules or sheets, but given that 60% of measurements in Day 7 cells is greater than 50 nm diameter, it seems likely that there is an increase in tubule diameter and an increase in formation of ER sheets [41], presumably to accommodate the increased protein synthesis (i.e., to provide room for ribosomes on the ER surface) and to create space for the folding machinery to assemble the Ig oligomers correctly. The crystalline nature of the ER contents apparent at high magnification was suggestive of ordered protein arrays, which might be expected to enable organized Ig folding and assembly. The concentrated spherical patterns in live ER are reminiscent of the whorls seen in cells overexpressing GFP chimeras [42]. These have been suggested as regions of segregation to protect the rest of the cell from potentially pathogenic membrane protein accumulation. However, in the case of B cells, this seems unlikely, as the ER proliferation is engendered to provide maximum Ig production capacity.

ERGIC-53 is a ubiquitously expressed lectin that acts as a cargo receptor to glycoproteins in the ER, facilitating their transition through the ER exit sites onto the Golgi [43]. *ERGIC-53* mRNA was found to up-regulate 18.5-fold in this study. In mammalian cell lines, ERGIC-53 is up-regulated during UPR through the ER stress response factor, ATF6 [19, 44, 45], but its role is unclear. Potentially, it could ensure that only correctly folded glycoproteins can proceed onto later compartments. A recent study has linked ERGIC-53 to Ig secretion, specifically through facilitating IgM polymerization, and has correlated up-regulated *ERGIC-53* expression with increased Ig production in murine splenocytes [20]. Whether ERGIC-53 up-regulation in differentiating B cells is merely a by-product of UPR induction or is related more directly to Ig secretion remains to be seen.

The differentiation of B cells provides an excellent model to study organelle biogenesis in the secretory pathway to aid understanding of how these specialized cells expand and reorganize organelles to accommodate the onset of Ig secretion. This system

will provide a useful basis for further investigation of regulatory components involved and their mechanism of action.

ACKNOWLEDGMENTS

Support is gratefully acknowledged: T. H. W. with a Royal Society Dorothy Hodgkin Fellowship and MRC New Investigator Award and S. J. K. with a MRC studentship. We thank Dr. David Stephens (University of Bristol) for his kind gift of the Sec24C antibody. We are grateful for the contributions of Dr. Maria McCrossan in the LSHTM electron microscopy facility, Carolynne Stanley for phlebotomy assistance, Liz King and Amir Horowitz for flow cytometry assistance, and Elizabeth Brooks, Grégoire Altan-Bonnet, Rachel Gregory, and Samantha Passey for technical assistance.

REFERENCES

1. King, L. B., Corley, R. B. (1989) Characterization of a presecretory phase in B-cell differentiation. *Proc. Natl. Acad. Sci. USA* **86,** 2814–2818.
2. Kirk, S. J., Ward, T. H. (2007) COPII under the microscope. *Semin. Cell Dev. Biol.* **18,** 435–447.
3. Sato, K., Nakano, A. (2007) Mechanisms of COPII vesicle formation and protein sorting. *FEBS Lett.* **581,** 2076–2082.
4. Jego, G., Bataille, R., Pellat-Deceunynck, C. (2001) Interleukin-6 is a growth factor for nonmalignant human plasmablasts. *Blood* **97,** 1817–1822.
5. Cobaleda, C., Schebesta, A., Delogu, A., Busslinger, M. (2007) Pax5: the guardian of B cell identity and function. *Nat. Immunol.* **8,** 463–470.
6. Calame, K. (2008) Activation-dependent induction of Blimp-1. *Curr. Opin. Immunol.* **20,** 259–264.
7. Reimold, A. M., Iwakoshi, N. N., Manis, J., Vallabhajosyula, P., Szomolanyi-Tsuda, E., Gravallese, E. M., Friend, D., Grusby, M. J., Alt, F., Glimcher, L. H. (2001) Plasma cell differentiation requires the transcription factor XBP-1. *Nature* **412,** 300–307.
8. Calfon, M., Zeng, H., Urano, F., Till, J. H., Hubbard, S. R., Harding, H. P., Clark, S. G., Ron, D. (2002) IRE1 couples endoplasmic reticulum load to secretory capacity by processing the *XBP-1* mRNA. *Nature* **415,** 92–96.
9. Van Anken, E., Romijn, E. P., Maggioni, C., Mezghrani, A., Sitia, R., Braakman, I., Heck, A. J. R. (2003) Sequential waves of functionally related proteins are expressed when B cells prepare for antibody secretion. *Immunity* **18,** 243–253.
10. Rousset, F., Peyrol, S., Garcia, E., Vezzio, N., Andujar, M., Grimaud, J-A., Banchereau, J. (1995) Long-term cultured CD40-activated B lymphocytes differentiate into plasma cells in response to IL-10 but not IL-4. *Int. Immunol.* **7,** 1243–1253.
11. O'Nions, J., Allday, M. J. (2004) Proliferation and differentiation in isogenic populations of peripheral B cells activated by Epstein-Barr virus or T cell-derived mitogens. *J. Gen. Virol.* **85,** 881–895.
12. Huggins, J., Pellegrin, T., Felgar, R. E., Wei, C., Brown, M., Zheng, B., Milner, E. C. B., Bernstein, S. H., Sanz, I., Zand, M. S. (2007) CpG DNA activation and plasma-cell differentiation of $CD27^-$ naive human B cells. *Blood* **109,** 1611–1619.
13. Crotty, S., Aubert, R. D., Glidewell, J., Ahmed, R. (2004) Tracking human antigen-specific memory B cells: a sensitive and generalized ELISPOT system. *J. Immunol. Methods* **286,** 111–122.
14. Ward, T. H. (2007) Trafficking through the early secretory pathway of mammalian cells. In *Protein Targeting Protocols* (M. van der Giezen, ed.), Totowa, NJ, USA, Humana, 281–296.
15. Vandesompele, J., De Preter, K., Pattyn, F., Poppe, B., Van Roy, N., De Paepe, A., Speleman, F. (2002) Accurate normalization of real-time quantitative RT-PCR data by geometric averaging of multiple internal control genes. *Genome Biol.* **3,** RESEARCH0034.
16. Bernales, S., McDonald, K. L., Walter, P. (2006) Autophagy counterbalances endoplasmic reticulum expansion during the unfolded protein response. *PLoS Biol.* **4,** e423.
17. Sciammas, R., Shaffer, A. L., Schatz, J. H., Zhao, H., Staudt, L. M., Singh, H. (2006) Graded expression of interferon regulatory factor-4 coordinates isotype switching with plasma cell differentiation. *Immunity* **25,** 225–236.
18. Kallies, A., Hasbold, J., Fairfax, K., Pridans, C., Emslie, D., McKenzie, B. S., Lew, A. M., Corcoran, L. M., Hodgkin, P. D., Tarlinton, D. M., Nutt, S. L. (2007) Initiation of plasma-cell differentiation is independent of the transcription factor Blimp-1. *Immunity* **26,** 555–566.
19. Nyfeler, B., Nufer, O., Matsui, T., Mori, K., Hauri, H-P. (2003) The cargo receptor ERGIC-53 is a target of the unfolded protein response. *Biochem. Biophys. Res. Commun.* **304,** 599–604.
20. Anelli, T., Ceppi, S., Bergamelli, L., Cortini, M., Masciarelli, S., Valetti, C., Sitia, R. (2007) Sequential steps and checkpoints in the early exocytic compartment during secretory IgM biogenesis. *EMBO J.* **26,** 4177–4188.
21. Hummeler, K., Harris, T. N., Tomassini, N., Hechtel, M., Farber, M. B. (1966) Electron microscopic observations on antibody-producing cells in lymph and blood. *J. Exp. Med.* **124,** 255–262.
22. Hearn, S. A., Silver, M. M., Sholdice, J. A. (1985) Immunoelectron microscopic labeling of immunoglobulin in plasma cells after osmium fixation and epoxy embedding. *J. Histochem. Cytochem.* **33,** 1212–1218.
23. Wiest, D. L., Burkhardt, J. K., Hester, S., Hortsch, M., Meyer, D. I., Argon, Y. (1990) Membrane biogenesis during B cell differentiation: most endoplasmic reticulum proteins are expressed coordinately. *J. Cell Biol.* **110,** 1501–1511.
24. Rambourg, A., Clermont, Y., Hermo, L., Chrétien, M. (1989) Formation of secretion granules in the Golgi apparatus of plasma cells in the rat. *Am. J. Anat.* **184,** 52–61.
25. Shaffer, A. L., Shapiro-Shelef, M., Iwakoshi, N. N., Lee, A-H., Qian, S-B., Zhao, H., Yu, X., Yang, L., Tan, B. K., Rosenwald, A., Hurt, E. M., Petroulakis, E., Sonenberg, N., Yewdell, J. W., Calame, K., Glimcher, L. H., Staudt, L. M. (2004) XBP1, downstream of Blimp-1, expands the secretory apparatus and other organelles, and increases protein synthesis in plasma cell differentiation. *Immunity* **21,** 81–93.
26. Skalet, A. H., Isler, J. A., King, L. B., Harding, H. P., Ron, D., Monroe, J. G. (2005) Rapid B cell receptor-induced unfolded protein response in nonsecretory B cells correlates with pro- versus antiapoptotic cell fate. *J. Biol. Chem.* **280,** 39762–39771.
27. Terasaki, M., Chen, L. B., Fujiwara, K. (1986) Microtubules and the endoplasmic reticulum are highly interdependent structures. *J. Cell Biol.* **103,** 1557–1568.
28. Hammond, A. T., Glick, B. S. (2000) Dynamics of transitional endoplasmic reticulum sites in vertebrate cells. *Mol. Biol. Cell* **11,** 3013–3030.
29. Shorter, J., Warren, G. (2002) Golgi architecture and inheritance. *Annu. Rev. Cell Dev. Biol.* **18,** 379–420.
30. Waterman-Storer, C. M., Salmon, E. D. (1998) Endoplasmic reticulum membrane tubules are distributed by microtubules in living cells using three distinct mechanisms. *Curr. Biol.* **8,** 798–806.
31. Wo'zniak, M. J., Bola, B., Brownhill, K., Yang, Y-C., Levakova, V., Allan, V. J. (2009) Role of kinesin-1 and cytoplasmic dynein in endoplasmic reticulum movement in VERO cells. *J. Cell Sci.* **122,** 1979–1989.
32. Vedrenne, C., Klopfenstein, D. R., Hauri, H-P. (2005) Phosphorylation controls CLIMP-63-mediated anchoring of the endoplasmic reticulum to microtubules. *Mol. Biol. Cell* **16,** 1928–1937.
33. Lu, L., Ladinsky, M. S., Kirchhausen, T. (2009) Cisternal organization of the endoplasmic reticulum during mitosis. *Mol. Biol. Cell* **20,** 3471–3480.
34. Guo, Y., Linstedt, A. D. (2006) COPII-Golgi protein interactions regulate COPII coat assembly and Golgi size. *J. Cell Biol.* **174,** 53–63.
35. Ward, T. H., Polishchuk, R. S., Caplan, S., Hirschberg, K., Lippincott-Schwartz, J. (2001) Maintenance of Golgi structure and function depends on the integrity of ER export. *J. Cell Biol.* **155,** 557–570.
36. Gürkan, C., Stagg, S. M., LaPointe, P., Balch, W. E. (2006) The COPII cage: unifying principles of vesicle coat assembly. *Nat. Rev. Mol. Cell Biol.* **7,** 727–738.
37. Sriburi, R., Jackowski, S., Mori, K., Brewer, J. W. (2004) XBP1: a link between the unfolded protein response, lipid biosynthesis, and biogenesis of the endoplasmic reticulum. *J. Cell Biol.* **167,** 35–41.
38. Lee, A-H., Iwakoshi, N. N., Glimcher, L. H. (2003) XBP-1 regulates a subset of endoplasmic reticulum resident chaperone genes in the unfolded protein response. *Mol. Cell. Biol.* **23,** 7448–7459.
39. Sriburi, R., Bommiasamy, H., Buldak, G. L., Robbins, G. R., Frank, M., Jackowski, S., Brewer, J. W. (2007) Coordinate regulation of phospholipid biosynthesis and secretory pathway gene expression in XBP-1(S)-induced endoplasmic reticulum biogenesis. *J. Biol. Chem.* **282,** 7024–7034.
40. Yoshida, H., Oku, M., Suzuki, M., Mori, K. (2006) pXBP1(U) encoded in XBP1 pre-mRNA negatively regulates unfolded protein response activator pXBP1(S) in mammalian ER stress response. *J. Cell Biol.* **172,** 565–575.
41. Voeltz, G. K., Prinz, W. A. (2007) Sheets, ribbons and tubules—how organelles get their shape. *Nat. Rev. Mol. Cell Biol.* **8,** 258–264.
42. Snapp, E. L., Hegde, R. S., Francolini, M., Lombardo, F., Colombo, S., Pedrazzini, E., Borgese, N., Lippincott-Schwartz, J. (2003) Formation of stacked ER cisternae by low affinity protein interactions. *J. Cell Biol.* **163,** 257–269.
43. Appenzeller-Herzog, C., Hauri, H-P. (2006) The ER-Golgi intermediate compartment (ERGIC): in search of its identity and function. *J. Cell Sci.* **119,** 2173–2183.
44. Spatuzza, C., Renna, M., Faraonio, R., Cardinali, G., Martire, G., Bonatti, S., Remondelli, P. (2004) Heat shock induces preferential translation of ERGIC-53 and affects its recycling pathway. *J. Biol. Chem.* **279,** 42535–42544.
45. Renna, M., Caporaso, M. G., Bonatti, S., Kaufman, R. J., Remondelli, P. (2007) Regulation of *ERGIC-53* gene transcription in response to endoplasmic reticulum stress. *J. Biol. Chem.* **282,** 22499–22512.

KEY WORDS:
endoplasmic reticulum · Golgi apparatus · immunoglobulin secretion · plasma cell · microscopy